INTERNATIONAL JOURNAL FOR NUMERICAL METHODS IN FLUIDS
Int. J. Numer. Meth. Fluids 2006; **51**:1407–1418
Published online 4 January 2006 in Wiley InterScience (www.interscience.wiley.com). DOI: 10.1002/fld.1170

An implicit Lagrangian lattice Boltzmann method for the compressible flows

Guangwu Yan*,†, Yinfeng Dong‡ and Yanhong Liu§

College of Mathematics, Jilin University, Changchun 130012, People's Republic of China

SUMMARY

In this paper, we propose a new Lagrangian lattice Boltzmann method (LBM) for simulating the compressible flows. The new scheme simulates fluid flows based on the displacement distribution functions. The compressible flows, such as shock waves and contact discontinuities are modelled by using Lagrangian LBM. In this model, we select the element in the Lagrangian coordinate to satisfy the basic fluid laws. This model is a simpler version than the corresponding Eulerian coordinates, because the convection term of the Euler equations disappears. The numerical simulations conform to classical results. Copyright © 2006 John Wiley & Sons, Ltd.

KEY WORDS: Lagrangian lattice Boltzmann method; displacement distribution functions; compressible flows

1. INTRODUCTION

The lattice Boltzmann method (LBM) has recently become an alternative method for computational fluid dynamics (CFD). Unlike conventional methods based on macroscopic continuum equation, the LBM starts from mesoscopic kinetic equations, i.e. the Boltzmann equation, to determine macroscopic fluid flows. The kinetic nature brings certain advantages over conventional numerical methods, such as its algorithmic simplicity, easy handing of complex boundary conditions, and efficient hydrodynamics simulations [1–5]. By using parallel computation

*Correspondence to: G. Yan, College of Mathematics, Jilin University, Changchun 130012, People's Republic of China.
† E-mail: yangw@email.jlu.edu.cn
‡ E-mail: dongyinfeng@sina.com.cn
§ E-mail: yanhong@mail.jlu.edu.cn

Contract/grant sponsor: Jilin University; contract/grant number: 985
Contract/grant sponsor: National Nature Science Foundation, China; contract/grant number: 10072023
Contract/grant sponsor: Chuangxin Foundation of Jilin University; contract/grant number: 2004CX041

Received 15 April 2005
Revised 4 November 2005
Accepted 7 November 2005

scheme in a multi-processor computer, we can easily solve a larger size of compressible flow problem with LBM.

During the past few years, much progress has been made in the development of the LBM [5]. Different models for simulating a wide variety of physical systems have been developed. In this article, we study a new method, Lagrangian LBM (LLBM). We will focus on the simulation of the shock waves and contact discontinuities in the Lagrangian coordinates.

There are many significant refined finite-difference methods for the compressible flows in history [6–12]. The total variation diminishing (TVD) [7] and the essentially non-oscillatory (ENO) [8] methods are to minimize numerical diffusions and non-physical oscillatory effects. The finite volume method with unstructured meshes is to fit complex boundaries [9]. The meshless method can get out the restriction of grid meshes [10]. Level set method can be used to trace the moving boundaries [11, 12]. When these schemes are applied to a shock wave tube problem, they produce a very high resolution for the shock, especially in TVD-type schemes. However, the contact discontinuity is still spread over typically three to four grid cells. For Eulerian finite-difference method, contact discontinuities are more difficult to compute with high resolution than in the case of shock since they do not have a natural compression mechanism to help their sharp numerical resolution. LBM can offer an ideal numerical effect and a new insight.

LBM is limited to low Mach flows [13], although several related compressible techniques have been proposed. In order to remove the low Mach restriction, in recent years, a series of lattice Boltzmann model for the compressible flows have been proposed [13–31]. Alexander *et al.* [13] chose a modified equilibrium distribution, allowing the sound speed small. Nadiga [14] proposed a discrete velocity model. Huang *et al.* [15] used flow-adapted discrete velocities, a non-unique equilibrium distribution constrained by a set of linear moments and the used interpolated nodes. Prendergast and Xu [16], Kim *et al.* [17], and Kotelnikov and Montgomery used Bhatnagar–Gross–Krook-type models [32] to establish new type flux and employed TVD flux limitation with the neighbourhood cells [18]. Renda *et al.* [19], Vahala *et al.* [20], Sun [21], De Cicco *et al.* [22], Yan *et al.* [23], Mason [24, 25] proposed many models by using additional techniques to achieve more higher Mach numbers for compressible flows.

These models encounter two problems to be solved: (1) the accuracy of these models are first-order system, (2) the solution of the shock is higher than the resolution of the contact discontinuity. In this paper, to overcome these problems, we propose a new method, LLBM. The Lagrangian forms are better suited to trace the discontinuity because it does not have convection term in the motion equations. Ancona defines a 'fully Lagrangian' LBM for the conservation system [26, 27], the main step in the approach is to use Lagrangian variables for the distribution function, and the lattice Boltzmann equation becomes the Lagrangian lattice Boltzmann equation. In this paper, the LLBM is proposed. It has three aspects that are different from Ancona's method: (i) using displacement distribution function instead of velocity distribution function. (ii) Macroscopic variables are mass, displacement and pressure forces, instead of density, momentum and energy. (iii) these equilibrium distribution functions are implicit formula related to the macroscopic variables in time step n and $n+1$. In the Lagrangian coordinates, the fluid consists of some elements with mass conservation only. These elements are 'large' fluid particles moving by pressure force. Since the element has one conservative variable, mass, the equilibrium distribution function is simpler than the corresponding Eulerian versions.

In the next section, the Lagrangian lattice Boltzmann model is described. In Section 3, we simulate four numerical examples with shock waves and contact discontinuities, and Section 4 gives concluding remarks.

2. LAGRANGIAN LATTICE BOLTZMANN MODEL

2.1. Lagrangian lattice Boltzmann equation

Let us define $f_\alpha(i,j,t)$ to be the displacement distribution function with micro-displacement e_α at time t and the Lagrangian coordinates (i,j). The Lagrangian coordinate (i,j) only takes on discrete values of the chosen lattice's nodes [26]. All the simulations shown in this paper have been done in two dimensions using a square HPP lattice [33], see Figure 1.

The nearest neighbour vectors are defined as

$$e_\alpha = \left(\cos\frac{\alpha-1}{2}\pi, \sin\frac{\alpha-1}{2}\pi\right), \quad \alpha = 1,\ldots,4 \tag{1}$$

The Lagrangian lattice Boltzmann equation for $f_\alpha(i,j,t)$ can be written as

$$\frac{\mathrm{d}f_\alpha(i,j,t)}{\mathrm{d}t} = \Omega_\alpha(i,j,t) \tag{2}$$

where $\Omega_\alpha(i,j,t)$ is the collision operator representing the rate of change of the distribution due to the collisions. According to Bhatnagar, Gross, and Krook (BGK), the collision operator is simplified using the single time relaxation approximation [18]. Hence, the Lagrangian lattice Boltzmann BGK equation is

$$\frac{\mathrm{d}f_\alpha(i,j,t)}{\mathrm{d}t} = \Omega_\alpha(i,j,t) = -\frac{1}{\tau}[f_\alpha(i,j,t) - f_\alpha^{\mathrm{eq}}(i,j,t)] \tag{3}$$

where $f_\alpha^{\mathrm{eq}}(i,j,t)$ is the equilibrium distribution with the Lagrangian coordinate (i,j), factor τ is the single relaxation time. The mass of per (i,j) is m, and macroscopic displacement, $X_\sigma(i,j,t)$ are defined in terms of the micro-displacement distribution function by

$$m(i,j,t) = \sum_\alpha f_\alpha(i,j,t) \tag{4}$$

$$m(i,j,t)X_\sigma(i,j,t) = \sum_\alpha f_\alpha(i,j,t)e_{\alpha\sigma} \tag{5}$$

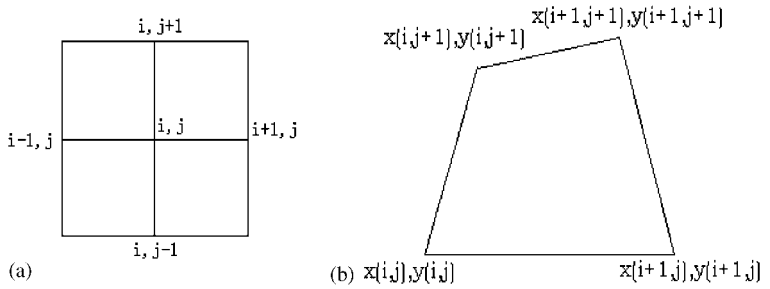

Figure 1. (a) HPP lattice on the Lagrangian coordinate; and (b) displacement.

In order to obtain a stable macroscopic mass m, we assume the equilibrium distribution function $f_\alpha^{\mathrm{eq}}(i,j,t)$ exists and

$$\sum_\alpha f_\alpha^{\mathrm{eq}}(i,j,t) = m(i,j,t) \tag{6}$$

At time step n, the collision term $\Omega_\alpha^n(i,j)$ is required to satisfy

$$\sum_\alpha \Omega_\alpha^n = 0 \tag{7}$$

$$\sum_\alpha \Omega_\alpha^n e_{\alpha j} = m\overline{u}_j^n \tag{8}$$

$$\sum_\alpha \frac{\Omega_\alpha^{n+1} - \Omega_\alpha^n}{\Delta t} e_{\alpha j} = \overline{N}_j^n \tag{9}$$

where n indicates time step, Δt is the time step length, $\overline{u}$ is the weight average velocity between time steps n and $n+1$, $\overline{N}$ is the weight average pressure-work between time steps n and $n+1$.

A suitable equilibrium distribution can be chosen in the following form for an implicit Lagrangian lattice Boltzmann scheme from Equations (7)–(9):

$$f_\alpha^{\mathrm{eq},n} = \frac{m}{b} + \frac{D}{bc^2} e_{\alpha\sigma}[mX_\sigma^n + \tau m\overline{u}_\alpha^n] \tag{10}$$

$$f_\alpha^{\mathrm{eq},n+1} = \frac{m}{b} + \frac{D}{bc^2} e_{\alpha\sigma}[mX_\sigma^{n+1} + \tau(m\overline{u}_\sigma^n + \overline{N}_\sigma^n \Delta t)] \tag{11}$$

In Equations (7) and (8), $b=4$ is the links number to the neighbourhood, $c=|e_\alpha|$, $D=2$ is the spatial dimensional number.

2.2. Macroscopic equations

In Equations (8) and (9), variables $\overline{u}_\sigma^n$, $\overline{N}_\sigma^n$ are the weight average time between n and $n+1$ of the velocity and pressure-work, that is

$$\overline{u}_\sigma^n = u_\sigma^n\theta + (1-\theta)u_\sigma^{n+1} \tag{12}$$

$$\overline{N}_\sigma^n = N_\sigma^n\theta + (1-\theta)N_\sigma^{n+1} \tag{13}$$

where θ is the parameter to control the explicit ($\theta=1$) or implicit ($\theta=0$) character of the scheme. Using Equations (7)–(9), we have

$$\Omega_\alpha^n = \frac{D}{bc^2} me_{\alpha\sigma}\overline{u}_\sigma^n \tag{14}$$

$$\Omega_\alpha^{n+1} = \frac{D}{bc^2}(m\overline{u}_\sigma^n + \Delta t\overline{N}_\sigma^n)e_{\alpha\sigma} \tag{15}$$

Summing Equation (2) over α and using conditions (4) and (7), we obtain the equation of conservation of mass

$$\frac{\mathrm{d}m}{\mathrm{d}t} = 0 \tag{16}$$

Using Equation (1) and then multiplying Equation (2) by the lattice vector $e_{\alpha\sigma}$ and summing over α gives the equation for the displacement

$$\frac{\mathrm{d}(mX_\sigma)}{\mathrm{d}t} = \sum_\alpha \Omega_\alpha^n e_{\alpha\sigma} = m\overline{u}_\sigma^n \tag{17}$$

Removing the mass m from two sides of Equation (17), we give the equation for relation of velocity and displacement

$$\frac{\mathrm{d}X_\sigma}{\mathrm{d}t} = \overline{u}_\sigma \tag{18}$$

Equation (2) can be written by first-order differential form

$$\frac{f_\alpha^{n+1} - f_\alpha^n}{\Delta t} = \Omega_\alpha^n + O(\Delta t) \tag{19}$$

by using Equations (11) and (19), we obtain the macroscopic dynamical equation in the condition of $\Delta t \to 0$,

$$\frac{\mathrm{d}^2(mX_\sigma)}{\mathrm{d}t^2} = \overline{N}_\sigma^n \tag{20}$$

In Equation (19), the distribution f_α^{n+1} is unknown as it contains the weight average time between n and $n+1$ of the velocity $\overline{u}_\sigma^n$ and pressure-work $\overline{N}_\sigma^n$, therefore, Equation (19) is an implicit equation, and has to be calculated in an iterative manner. Another condition, isentropic equation, can be used to modify the convergence of the implicit equations.

2.3. An implicit scheme with entropy modification [*34*]

We consider isentropic flows: the entropy of each computational element is written as

$$S = \frac{p}{\rho^\gamma} \tag{21}$$

where ρ is the density, γ is the specific heat ratio. Consider the isentropic flow, we have

$$\frac{\mathrm{d}S}{\mathrm{d}t} = 0 \tag{22}$$

The density ρ of the fluid can be written as

$$\rho = \frac{M}{\Lambda_{i,j}} \tag{23}$$

where M is the element mass. The volume of the element given by

$$\Lambda_{i,j} = 0.5[(x_{i,j} - x_{i+1,j+1})(y_{i+1,j} - y_{i,j+1}) - (x_{i+1,j} - x_{i,j+1})(y_{i,j} - y_{i+1,j+1})] \tag{24}$$

The mass in the lattice i,j is defined by the average mass of its four neighbouring elements, given by

$$m_{i,j} = \tfrac{1}{4}[\Lambda_{i-1,j-1}\rho_{i-1,j-1} + \Lambda_{i,j-1}\rho_{i,j-1} + \Lambda_{i,j}\rho_{i,j} + \Lambda_{i-1,j}\rho_{i-1,j}] \tag{25}$$

In the lattice i,j, the pressure-works $N_{xi,j}$ and $N_{yi,j}$ are calculated as

$$N_{xi,j} = \tfrac{1}{2}[p_{i,j}(y_{i+1,j} - y_{i,j+1}) + p_{i-1,j}(y_{i,j+1} - y_{i+1,j}) + p_{i-1,j-1}(y_{i-1,j} - y_{i,j-1}) + p_{i,j-1}(y_{i,j-1} - y_{i+1,j})] \quad (26)$$

$$N_{yi,j} = \tfrac{1}{2}[p_{i,j}(x_{i,j+1} - x_{i+1,j}) + p_{i-1,j}(x_{i-1,j} - x_{i,j+1}) + p_{i-1,j-1}(x_{i,j-1} - x_{i-1,j}) + p_{i,j-1}(x_{i+1,j} - x_{i,j+1})] \quad (27)$$

The iteration procedure in this paper can be given as

(1) Calculate f_α^n from macroscopic variable.
(2) Assign updated F_α as f_α^{n+1}, we get Ω_α^n from Equation (19), X_σ from Equation (5), $\overline{u}_\alpha$ from Equation (10), u_σ^{n+1} from Equation (12).
(3) Assign updated $\overline{p}$ as p^{n+1}, we calculated $N_{xi,j}^{n+1}$, $N_{yi,j}^{n+1}$ from Equations (26) and (27), $\overline{N}_{xi,j}^{n+1}$, $\overline{N}_{yi,j}^{n+1}$ from Equation (13), Ω_α^{n+1} from Equation (15).
(4) Calculate f_α^{n+1} from Equation (19), X_σ from Equation (5).
(5) Calculate Λ_α^{n+1} from Equation (24), $p_{i,j}^{n+1}$ from Equation (23).
(6) Check the convergence of pressures. If $|(p_{i,j}^{n+1} - \overline{p})/p_{i,j}^{n+1}| < \delta_1$ is satisfied, go to step (7); otherwise go to step (3).
(7) Check the convergence of the condition. If $|(f_\alpha^{n+1} - F)/f_\alpha^{n+1}| < \delta_2$ is satisfied, begin to calculate the next time step; otherwise go to step (2).

In the case of a one-dimensional domain, it leads to

$$N_i = -(p_i - p_{i-1}), \quad \Lambda_i = x_{i+1} - x_i, \quad m_i = \tfrac{1}{2}(M_i + M_{i+1}) \quad (28)$$

and the coefficient D/bc^2 in f_α^{eq} becomes $1/bc^2$.

3. NUMERICAL EXAMPLES

In this section, we apply the LLBM to four gas flows. The first one is the typical Riemann problem, namely the shock tube problem of Lax. The second one is the propagation of a planar pressure pulse [34]. The third one simulates the response of a planar flame to a harmonic pressure wave [34]. The last problem is two-dimensional Sod's problem containing shock waves

1. One-dimensional Lax's problem [23].

In Lax's problem, the initial condition (at $t = 0.0$) is defined by

$$\begin{aligned} (\rho, u, p) &= (0.445, 0.698, 3.528) \quad \text{if} \quad 0 \leqslant x \leqslant 0.5 \\ (\rho, u, p) &= (0.5, 0.0, 0.571) \quad \text{if} \quad 0.5 < x \leqslant 1.0 \end{aligned} \quad (29)$$

Figure 2(a)–(d) displays the results of the density ρ, pressure p, velocity u and the internal energy E calculated by using LLBM at the time $t = 100\Delta t$. Numerical experiments showed that for Lax's problem the time step is $\Delta t = 4.8387 \times 10^{-3}$. The boundary condition at the two

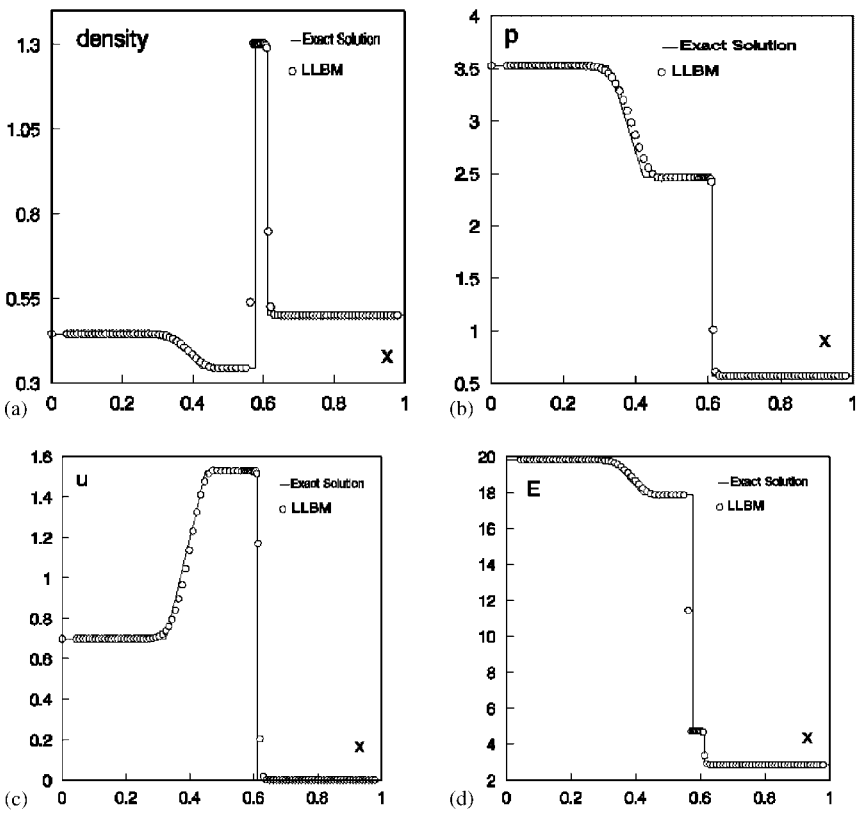

Figure 2. Comparison of exact solutions and LLBM results of one-dimensional Lax's problem. (a)–(d) (solid lines are exact solutions, circle are LLBM results): (a) density; (b) pressure; (c) velocity; and (d) internal energy. Parameters: $\Delta t = 4.8387 \times 10^{-4}$, lattice size $N = 100$, time $t = 100\Delta t$, $\gamma = 1.4$, $b = 2$, $c = 0.01$, $\tau = 1.2$, $\theta = -1.2$.

ends is the Von Neumann condition. The internal energy E can be calculated by $E = p/\rho(\gamma - 1)$. By comparing this results with the exact solution, we find the shock waves and the contact discontinuities spread over typically two to three grid cells. This method is slightly higher resolution than the LBM method [23].

2. One-dimension pressure wave propagation [34].

In this example, the initial pressure pulse will break into two propagating waves in the positive and negative directions. We select the initial conditions in the region $x \in [0, 1]$

$$\rho(x) = 0, \quad u(x) = 0, \quad p(x) = 1.0 + 0.5 \times \mathrm{sech}[50(x - 50)] \tag{30}$$

Figure 3(a) is the initial pressure. Figure 3(b)–(d) displays the results of the pressure p, density ρ, and velocity u at the time $t = 500\Delta t$. The results of the LLBM calculation can be compared with Liu's results in Reference [34]. This scheme can maintain these strong gradients.

3. One-dimension response of a planar flame to a harmonic pressure wave.

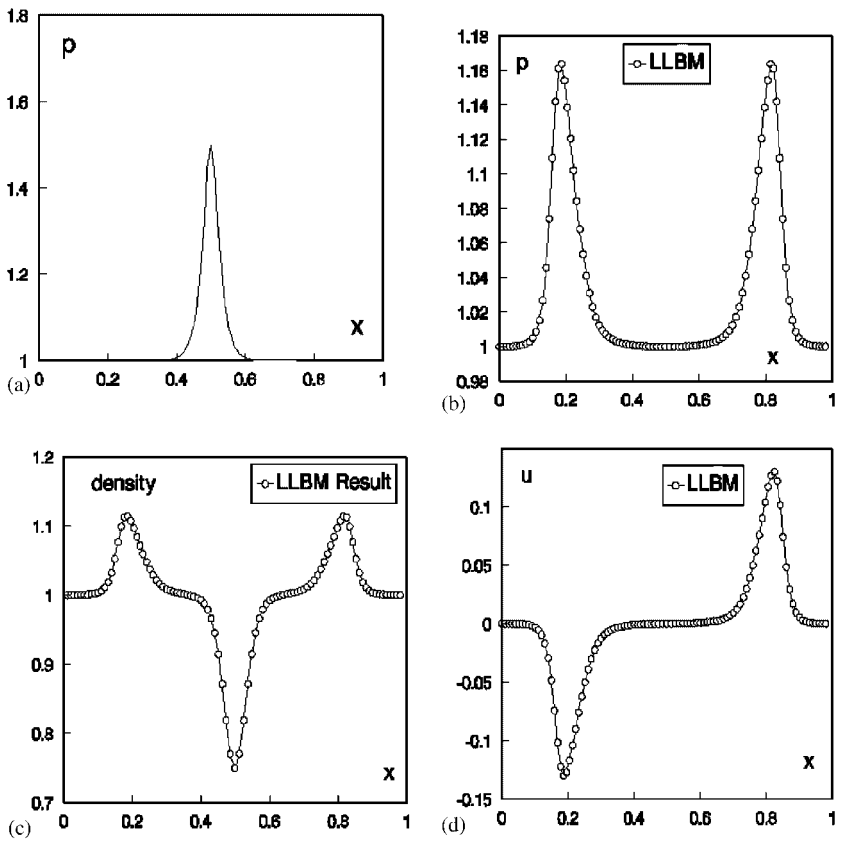

Figure 3. Numerical results of one-dimensional pressure wave propagation: (a) Initial pressure. (b)–(d) (LLBM results); (b) pressure; (c) density; and (d) velocity. Parameters are $\Delta t = 4.84 \times 10^{-4}$, element number $N = 100$, time $t = 500\Delta t$, $\gamma = 1.4$, $b = 2$, $c = 0.01$, $\tau = 1.2$, $\theta = -1.2$.

Example 3 is a one-dimension response of planar flame to a harmonic pressure wave with the following initial data:

$$u(x) = 0 \quad \text{for } x \in [0, 2.0] \tag{31}$$

$$\begin{aligned} \rho(x) &= 0.2 \quad \text{if } 0 \leqslant x \leqslant 1.5 \\ \rho(x) &= 1.0 \quad \text{if } 1.5 < x \leqslant 2.0 \end{aligned} \tag{32}$$

$$\begin{aligned} p(x) &= 1.0 \quad \text{if } 0 \leqslant x \leqslant 0.9 \text{ or } 1.5 \leqslant x \leqslant 2.0 \\ p(x) &= 1.0 + 0.2 \sin\left[\frac{\pi}{0.3}(x - 1.2)\right] \quad \text{if } 0.9 < x \leqslant 1.5 \end{aligned} \tag{33}$$

The problem arises from the study of the interaction at the very early stage between a planar premixed flame and a long length-scale pressure wave. On an acoustic time scale,

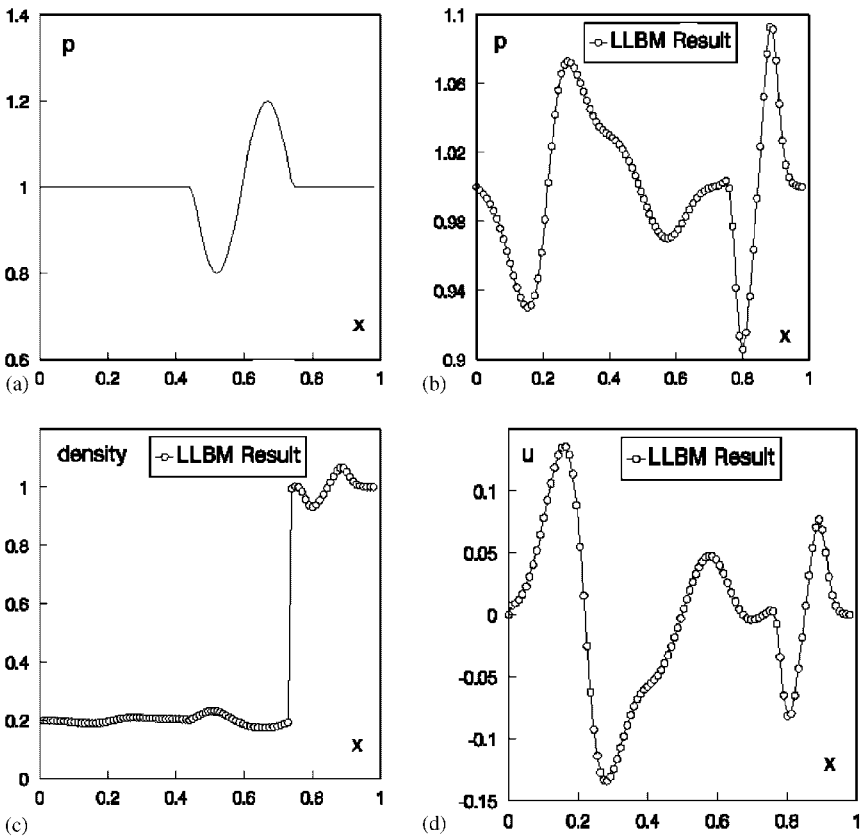

Figure 4. Numerical results of one-dimensional flame pressure wave: (a) Initial pressure. (b)–(d) (LLBM results); (b) pressure; (c) density; and (d) velocity. Parameters: $\Delta t = 4.84\times10^{-4}$, element number $N = 100$, time $t = 300\Delta t$, $\gamma = 1.4$, $b = 2$, $c = 0.01$, $\tau = 1.2$, $\theta = -1.2$.

the planar flame front can be treated as a density discontinuity and a gas flow driven by a pressure disturbance.

Figure 4(a) is the initial pressure. Figure 4(b)–(d) displays the results of the pressure p, density ρ, and velocity u at the time $t = 300\Delta t$. The time step is $\Delta t = 4.84\times10^{-3}$. The boundary condition at the two ends is the Von Neumann condition. The result of this example shows that LLBM can remove the numerical instabilities caused by the negative dissipation in Reference [34] and LLBM can be used to compute the density discontinuity problems.

4. Two-dimensional circular version of Sod's problem.

In order to evaluate the capability of the LLBM, we first apply the LLBM to simulate two-dimensional gas-dynamics problem, two-dimensional circular version of the Sod's problem. The initial conditions are the region of high pressure and high density. In this case it is a circle of radius 0.15 centred at $(0.5, 0.5)$ with $V = 0$ everywhere. This flow consists of three waves, an outward travelling shock followed by a contact discontinuity and a rarefaction travelling

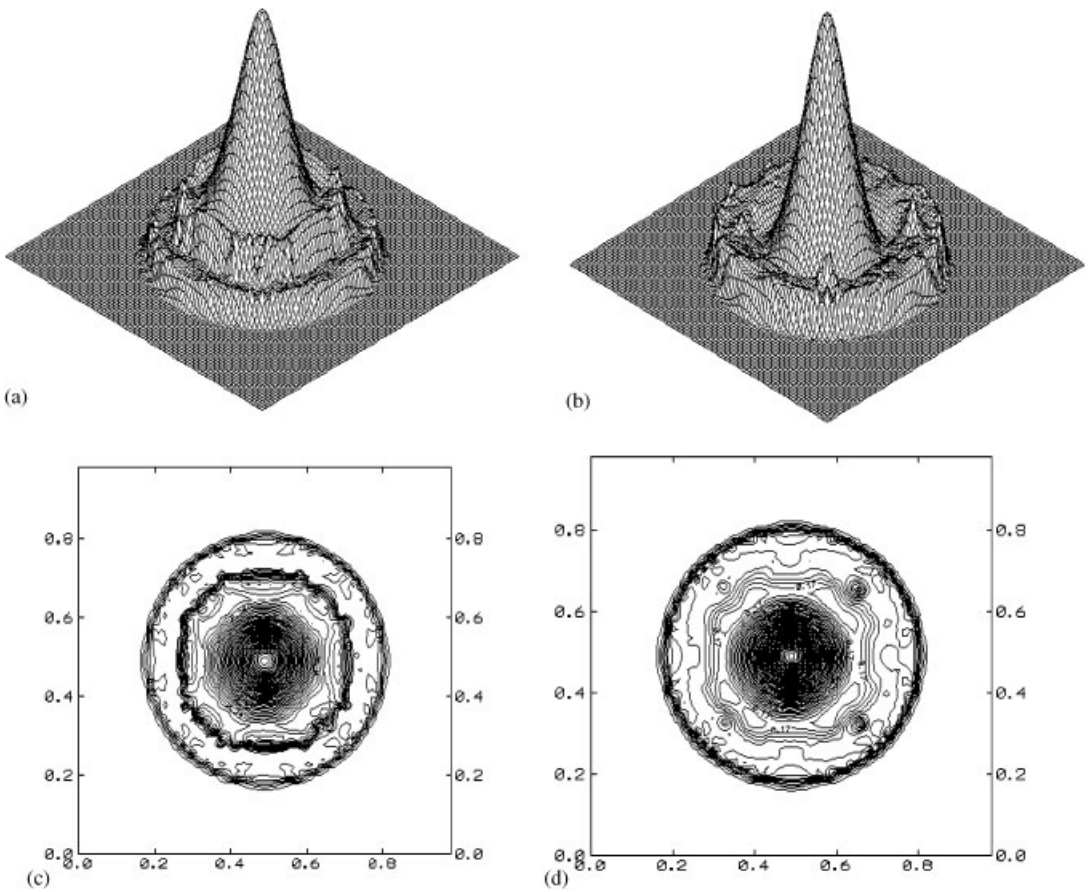

Figure 5. Numerical results of two-dimensional Sod's problem. (a) and (b) Density and pressure profiles at $t=100\Delta t$. (c) and (d) Contour lines of the density and pressure. Parameters: $\Delta t=1.0\times10^{-3}$, lattice size 100×100, time $t=100\Delta t$, $\gamma=1.4$, $b=4$, $c=20.0$, $\tau=1.2$, $\theta=-1.2$. The contour lines number is 50.

toward the centre. That is,

$$\begin{aligned} &\rho=1.0, \quad u=0.0, \quad p=1.0 \qquad \text{if } (x-0.5)^2+(y-0.5)^2\leqslant 0.15^2 \\ &\rho=0.125, \quad u=0.0, \quad p=0.1 \quad \text{if } (x-0.5)^2+(y-0.5)^2\geqslant 0.15^2 \end{aligned} \tag{34}$$

The solution domain $[0,1]\times[0,1]$ is divided into 100×100 squares. Parameters: time step $\Delta t=1.0\times10^{-3}$, $\gamma=1.4$, $b=4$, $c=20.0$, $\tau=1.2$, $\theta=-1.2$. In Figure 5(a) and (b), we plot the density and pressure profiles at $t=100\Delta t$. Figure 5(c) and (d) is contour lines of the density and the pressure. We find a large gradient region in the profiles and the contour lines. In Figure 4(a) and (c), the shock wave is the outside large gradient ring, the contact discontinuity is the inner large gradient ring. They are reasonably good for two-dimensional shock waves and contact discontinuities. We find two drawbacks in the results, (1) profiles of density and pressure possess dissymmetrical ring, (2) contact discontinuity is smoothless.

In the first case, the HPP lattice causes the drawback. The HPP lattice lacks of enough symmetry, the FHP lattice [1] is a suitable choice. The second case may be overcome by adjusting those parameters to improve the viscosity of the scheme.

4. CONCLUDING REMARKS

We have proposed an implicit LLBM for the compressible flows. Unlike standard LBM approaches which use Eulerian coordinates to solve macroscopic governing equations, our scheme is based on the Lagrangian coordinates and Newton's second law to build the motive equation of the elements. The shock waves and contact discontinuities can be automatically emerged. Using the implicit scheme, we obtained good numerical simulation, which are effective enough in the resolution of the shock wave and contact discontinuity.

In this paper, the LLBM has two advantages in contrast to Eulerian version: (i) The energy equation or entropy equation is vanished, and the energy and entropy equation are complex to modelling moments of equilibrium distribution function. In this paper, we assume the flows as isentropic flow. (ii) The LLBM does not have convection term. It makes the Lagrangian lattice Boltzmann easily modelled for the compressible flows.

Finally, we point out that some problems to be solved: (1) accuracy and stability of the lattice Lagrangian method, (2) the boundary condition on the wall, (3) the possibility to develop LLBM for dissymmetrical flows, and (4) treat examples with Mach numbers. We will discuss these problems in further papers.

ACKNOWLEDGEMENTS

This work was supported by Jilin University (Grant No. 985), the National Nature Science Foundation of China (Grant No. 10072023), and the Chuangxin Foundation of Jilin University (No. 2004CX041). We would like to thank Prof Yuan Li, Prof Wang Jianping, and Dr Yang Hua for their many helpful suggestions.

REFERENCES

1. Frisch U, Hasslacher B, Pomeau Y. Lattice gas automata for the Navier–Stokes equations. *Physical Review Letters* 1986; **56**:1505–1508.
2. Qian YH, d'humieres D, Lallemand P. Lattice BGK model for Navier–Stokes equations. *Europhysics Letters* 1992; **17**(6):479–484.
3. Chen HD, Chen SY, Matthaeus MH. Recovery of the Navier–Stokes equations using a lattice Boltzmann method. *Physical Review A* 1992; **45**:5339–5342.
4. Benzi R, Succi S, Vergassola M. The lattice Boltzmann equations: theory and applications. *Physics Reports* 1992; **222**:147–197.
5. Chen SY, Doolen GD. Lattice Boltzmann method for fluid flows. *Annual Review of Fluid Mechanics* 1998; **3**:314–322.
6. Woodward P, Colella P. The numerical simulations of two-dimensional fluid flow with strong shocks. *Journal of Computational Physics* 1984; **54**:115–174.
7. Harten A. On a class of high resolution total variation stable finite difference schemes. *SIAM Journal on Numerical Analysis* 1984; **21**:1–23.
8. Harten A, Engquist B, Osher S, Chakravathy R. Uniformly high order accurate essentially non-oscillatory schemes, III. *Journal of Computational Physics* 1997; **131**:3–47.
9. Versteeg HK, Malalasekera W. *An Introduction to Computational Fluid Dynamics—The Finite Volume Method*. Longman Group Ltd: Harlow, U.K., 1995.
10. Zhang LT, Wagner GJ, Liu WK. A parallelized meshfree method with boundary enrichment for large-scale CFD. *Journal of Computational Physics* 2002; **176**:483–506.

11. Sethian JA. Theory, algorithms, and applications of level set methods for propagating interface. *Acta Numerica* Cambridge University Press: Cambridge, U.K., 1995.
12. Grasso F, Meola C. Euler and Navier–Stokes equations for compressible flows: finite-volume method. In *Handbook of Computational Fluid Mechanics*, Pryret R (ed.). Academic Press: San Diego, 1996.
13. Alexander FJ, Chen H, Chen S *et al.* Lattice Boltzmann model for compressible fluids. *Physical Review A* 1992; **46**:1967–1970.
14. Nadiga BT. An Euler solver based on locally adaptive discrete velocities. *Journal of Statistical Physics* 1995; **81**:129–146.
15. Huang J, Xu F, Vallieres M *et al.* A thermal LBGK model for large density and temperature difference. *International Journal of Modern Physics C* 1997; **8**:827–841.
16. Prendergast KH, Xu K. Numerical hydrodynamics from gas-kinetic theory. *Journal of Computational Physics* 1993; **109**:53–66.
17. Kim C, Xu K, Martinelli L *et al.* Analysis and implementation of the gas kinetic BGK scheme for computing inhomogeneous fluid behavior. *International Journal for Numerical Methods in Fluids* 1997; **25**:21–49.
18. Kotelnikov AD, Montgomery DC. A kinetic method for computing inhomogeneous fluid behavior. *Journal of Computational Physics* 1997; **134**:364–388.
19. Renda A, Bella G, Succi S *et al.* Thermo hydrodynamics lattice BGK schemes with non-perturbative equilibrium. *Europhysics Letters* 1998; **41**:279–283.
20. Vahala G, Pavlo P, Vahala L *et al.* Thermal lattice Boltzmann models (TLBM) for compressible flows. *International Journal of Modern Physics C* 1998; **9**:1247–1261.
21. Chenghai S. Lattice-Boltzmann model for high speed flows. *Physical Review E* 1998; **58**:7283–7287.
22. De Cicco M, Succi S, Balla G. Nonlinear stability of compressible thermal lattice BGK model. *SIAM Journal on Scientific Computing* 1999; **21**:366–377.
23. Yan GW, Chen YS, Hu SX. Simple lattice Boltzmann model for simulating flows with shock wave. *Physical Review E* 1999; **59**:454–459.
24. Mason RJ. A compressible lattice Boltzmann model. *Bulletin of the American Physical Society* 2000; **45**: 168–170.
25. Mason RJ. A Multi-speed compressible lattice Boltzmann model. *Journal of Statistical Physics* 2002; **107**: 385–400.
26. Ancona MG. Fully-Lagrangian and lattice Boltzmann methods for solving systems of conservation equations. *Journal of Computational Physics* 1994; **115**:107–120.
27. Yang Y, Huang JC. Rarefied flow computational using nonlinear model Boltzmann equations. *Journal of Computational Physics* 1995; **120**:323–339.
28. Mieussens L. Discrete-velocity models and numerical schemes for the Boltzmann-BGK equation in plane and axisymmetric geometries. *Journal of Computational Physics* 2000; **162**:429–466.
29. Luo LS. Some recent results on discrete velocity models and ramifications for lattice Boltzmann equation. *Computer Physics Communications* 2000; **162**:63–74.
30. He XY, Chen SY, Doolen GD. A novel thermal model for the lattice Boltzmann method incompressible limit. *Computer Physics Communications* 1997; **146**:282–300.
31. Struchtrup H. The BGK model or an ideal gas with an internal degree of freedom. *Transport Theory and Statistical Physics* 1999; **28**:369–385.
32. Bhatnagar PL, Gross EP, Krook M. A model for collision processes in gases. *Physical Review* 1954; **94**(3): 511–525.
33. Hardy J, Pomeau Y, de Pazzis O. Time evolution of two-dimensional model system. I. Invariant states and time correlation functions. *Journal of Mathematical Physics* 1973; **14**:1746–1759.
34. Liu F, McIntosh AC, Brindley J. An implicit Lagrangian method for solving one and two-dimensional gasdynamic equations. *Journal of Computational Physics* 1994; **110**:112–133.

